

Original citation:

Bruen, Thomas, Marco, James and Gama, Miguel (2014) Current variation in parallelized energy storage systems. In: Vehicle Power and Propulsion Conference 2014 (VPPC 2014), Portugal, 27-30 Oct 2014. Published in: Proceedings of the 10th Vehicle Power and Propulsion Conference 2014 pp. 1-6. (In Press)

Permanent WRAP url:

<http://wrap.warwick.ac.uk/64039>

Copyright and reuse:

The Warwick Research Archive Portal (WRAP) makes this work of researchers of the University of Warwick available open access under the following conditions. Copyright © and all moral rights to the version of the paper presented here belong to the individual author(s) and/or other copyright owners. To the extent reasonable and practicable the material made available in WRAP has been checked for eligibility before being made available.

Copies of full items can be used for personal research or study, educational, or not-for-profit purposes without prior permission or charge. Provided that the authors, title and full bibliographic details are credited, a hyperlink and/or URL is given for the original metadata page and the content is not changed in any way.

Publisher's statement:

A note on versions:

The version presented in WRAP is the published version or, version of record, and may be cited as it appears here.

For more information, please contact the WRAP Team at: publications@warwick.ac.uk



<http://wrap.warwick.ac.uk/>

Current variation in parallelized energy storage systems

Thomas Bruen, James Marco
International Digital Laboratory
WMG, University of Warwick
Coventry, United Kingdom
thomas.bruen@warwick.ac.uk
james.marco@warwick.ac.uk

Miguel Gama
Jaguar Land Rover
Coventry, United Kingdom
mgamaval@jaguarlandrover.com

Abstract— an electric vehicle battery pack may employ cells connected electrically in parallel to meet energy and power requirements. For the battery management system, cells connected in parallel are often treated as a single larger component. However, research has identified that the state of charge and cell current may not be equal due to differences in capacity, impedance and cell temperature. In this paper, the authors develop a parallel cell model validated against experimental data. The model is used to evaluate cell energy variation and the impact this can have on the design of highly parallelized battery systems.

Keywords—lithium-ion, battery, Battery Management System, BMS, parallel cells, EV, HEV, equivalent circuit model

I. INTRODUCTION

From the perspective of a battery management system (BMS), individual cells connected electrically in parallel are often considered to be one larger capacity cell with a single value of state of charge (SOC) [1], due to the unit operating at one voltage, the individual cell currents not being measured and the tendency for cells in parallel to self-balance over time. However, there will be variations in cell performance caused by two main effects. Differences in cell impedance and energy capacity will cause an unequal current distribution, with different open circuit voltages (OCVs) and impedance values having to resolve current in such a way that the terminal voltage is common for each cell. Secondly, the resistance of the bus bars connecting the cells can create a voltage drop between each parallel loop. Research by [2] showed that cells closest to the current source were prone to higher current flow than those furthest away from the source, resulting in different SOC's over time.

These issues combined present a number of challenges for the BMS. The different capacities and current flows within a parallel unit mean that the SOC of the individual cells may not be equal. A single cell model of the parallel unit will have one SOC, but the relationship of this SOC to the individual cell SOC is not well defined. A single model of parallel cells was developed by [3], but this assumed that the cells were identical which in reality may not be true because of ageing [4] and extrinsic factors such as temperature [5]. Cells may age at different rates specifically because of parallelization, due to the

different current throughput and the resultant temperature gradients. Research by [6] showed that a 20% mismatch of internal resistance in 18650 type lithium ion cells resulted in a 40% reduction in cycle life due to increased capacity fade. Recent work in [7] also suggests that when cells at different levels of ageing are connected in parallel, ageing is accelerated.

As cell currents are not monitored, there is a danger of some cells exceeding current limits even though the nominal current (i.e. the applied current divided by the number of cells) is within the manufacturer's specifications. Similarly, individual cells may go beyond limits on SOC imposed by the BMS to reduce the effects of ageing, leading to the battery pack reaching its end of life prematurely. Finally, due to the passive nature of the electrical interconnection between adjacent cells, there is typically no control over how the applied current is distributed between cells; this may reduce the effectiveness of the balancing system when trying to reduce the voltage or SOC difference between parallel units in series.

In this paper, equivalent circuit models (ECMs) are outlined and a method of combining the ECMs in a parallel configuration is proposed. ECMs are created from experimental data for four cells of the same type but at different states of ageing, allowing for analysis of interaction between cells with different resistance and capacity values, which can occur through factors such as temperature gradients, as well as ageing. Using this model, a dynamic vehicle cycle, and large depth of discharge (DOD) cycle are simulated, and the impact of connection resistance between parallel cells and the case of a cell being disconnected are both evaluated. From this, conclusions can be drawn about the variation in performance that is not seen by a BMS.

II. CELL MODELLING

The ECM for a single cell is presented first, and then extended to a general case of a number of cells in parallel.

A. Single Cell Model

An ECM is commonly used to simulate cells due to their ease of parameterization and real time capability [8]. The model consists of a variable voltage source to represent OCV as a function of SOC, a resistor to capture the DC resistance of the

The research presented within this paper is supported by the UK Technology Strategy Board (TSB) through the WMG Centre High Value Manufacturing (HVM) Catapult in collaboration with Jaguar Land Rover.

cell, and a resistor and capacitor connected in parallel (RC pair) to capture dynamics. The number of RC pairs can be increased for improved bandwidth at the expense of increased complexity. The equations that govern the ECM response are given in (1)-(4). Equation (1) governs the response of a single RC pair, and the parameters are a function of SOC. v_p is the polarization voltage over the RC pair, R_p and C_p are the RC pair resistance and capacitance respectively, R_{DC} is the DC resistance, v_{OC} is the OCV, i_{cell} is the current applied to the cell, Q is the cell capacity in Ah, n_{RC} is the number of RC pairs, and v_t is the voltage over the cell terminals.

$$\dot{v}_p = \frac{-v_p}{R_p C_p} + \frac{i_{cell}}{C_p} \quad (1)$$

$$SOC = 100 \frac{i_{cell}}{3600Q} \quad (2)$$

$$v_{OC} = f(SOC) \quad (3)$$

$$v_t = v_{OC} + \sum_{n=1}^{n_{RC}} v_p(n) + R_{DC} i_{cell} \quad (4)$$

B. Parallel Cell Model

Connecting cells in parallel adds additional constraints to the model: terminal voltage is common to all cells and the cell currents sum up to the source current. This algebraic constraint changes the cell from a system of ODEs to a system of DAEs of index 1. The equations for the system have been derived by using mesh analysis to consider cells connected with (optional) connection resistances, as shown in Figure 1. For brevity the example presented here uses one RC pair, but the solution can be extended to several. This system is now a set of differential-algebraic equations (DAEs).

The equations from section II A still apply, but with the cell current given by (5).

$$i_{cell\ n} = i_n - i_{n+1}; \quad i_{cell\ N} = i_N \quad (5)$$

The voltages around each loop must sum to zero, as per Kirchoff's voltage law in (6), where R_c is the inter-cell connection resistance.

$$v_{OC\ n} - v_{OC\ n-1} + v_{d\ n} - v_{d\ n-1} + R_{0\ n}(i_n - i_{n+1}) - R_{0\ n-1}(i_{n-1} - i_n) + 2R_c i_n = 0 \quad (6)$$

This can be put into matrix form, as in (7), where \mathbf{A} is the system jacobian and \mathbf{B} is the input vector. The first loop current i_1 is the source current and so is a model input not a state variable.

$$\begin{bmatrix} \dot{SOC}_1 \\ v_{p\ 1} \\ 0 \\ \dot{SOC}_2 \\ \vdots \\ 0 \\ \dot{SOC}_N \\ v_{p\ N} \end{bmatrix} = [\mathbf{A}] \begin{bmatrix} SOC_1 \\ v_{p\ 1} \\ i_2 \\ SOC_2 \\ \vdots \\ i_N \\ SOC_N \\ v_{p\ N} \end{bmatrix} + [\mathbf{B}] i_1 \quad (7)$$

This has been solved using the ode15s variable-step solver in MATLAB.

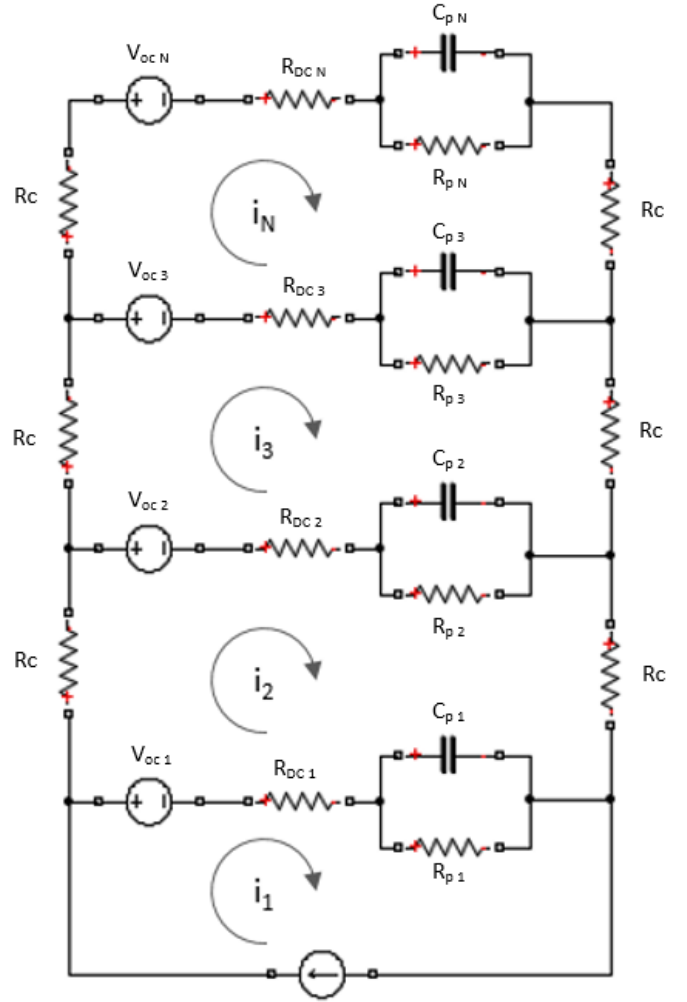


Figure 1: Schematic of parallel connected cells

III. CELL DATA GENERATION

Experimental data were collected for four 3Ah 18650-type lithium ion cells, and used to parameterize the ECMs.

A. Ageing

The cells were aged by different amounts in order to better observe interactions between cell impedance and capacity. The ageing profile is shown in Figure 2 and involved repeated cycles of the following: a 1C discharge until the lower voltage limit was reached followed by CC-CV charging at $C/2$ to the upper cell voltage limit, with a $C/20$ cut-off current.

The four cells were aged by 0, 50, 100 and 150 cycles respectively. Electrochemical impedance spectroscopy (EIS) tests were performed between 10mHz and 100kHz to analyze how the cells have aged. For clarity the EIS data presented in this paper have been reduced to below 1kHz as the higher frequency inductive region is not considered for this analysis.

Example results are shown in Figure 3 and summarized in Table 1. Two metrics are considered: DC resistance, where the impedance line crosses the real axis, and diffusive resistance, which is taken to be resistance up to the turning point where the Warburg region begins[9]. These regions are shown on Figure 3.

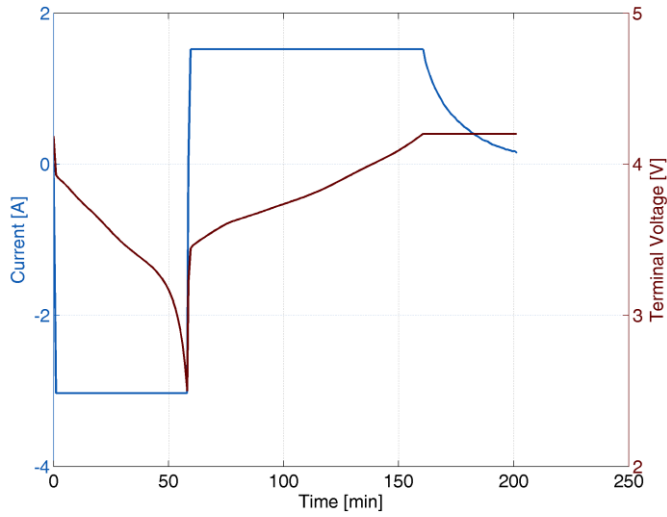


Figure 2: Discharge-charge cycle used for cell ageing

TABLE I. SUMMARY OF EIS RESULTS AT 50% SOC

Cell	Crossing Frequency (Hz)	DC Resistance (mΩ)	Turning Frequency (Hz)	Diffusive Resistance (mΩ)
0 Ageing Cycles	611.6	31.52	0.398	46.32
50 Ageing Cycles	496.4	32.27	0.200	51.17
100 Ageing Cycles	502.0	32.62	0.126	58.20
150 Ageing Cycles	511.3	32.97	0.100	63.13
Four cells in Parallel	353.2	8.33	0.158	13.64

B. Characterization

Characterization tests were performed to evaluate their performance and to create an ECM. To simplify the analysis, all tests were performed at 25°C to remove the effect of temperature on ECM parameters. Cell capacity was measured at 1C, and a pseudo OCV-SOC curve obtained by discharging the cell at C/25.

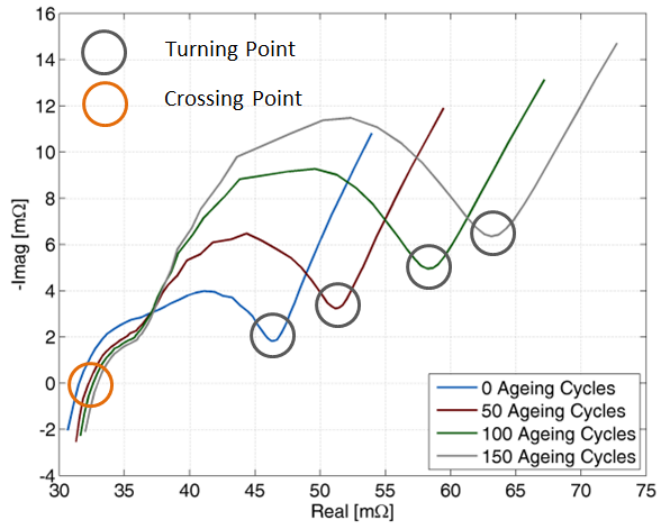


Figure 3: Nyquist plot of impedance for differentially aged cells

Cell dynamics were evaluated using a pulse power profile of 10s current followed by 5 minutes resting, and EIS tests. Figure 4 shows how the diffusive resistance for each cell varies as a function of SOC. For this particular cell, there was little change in DC resistance with SOC.

The cells were characterized in series and parallel. The impedance of the individual cells can be parallelized and compared to the physically connected cell, using (8), where Z is the impedance and N the number of cells in parallel.

$$Z = \frac{1}{\sum_{n=1}^N \frac{1}{Z_n}} \quad (8)$$

The results show that the physically connected cell has a slightly higher resistance, which may be due to increased connection resistance in the experimental setup. However, there does not appear to be any significant interaction between the cells that cannot be captured using single cell models connected in parallel.

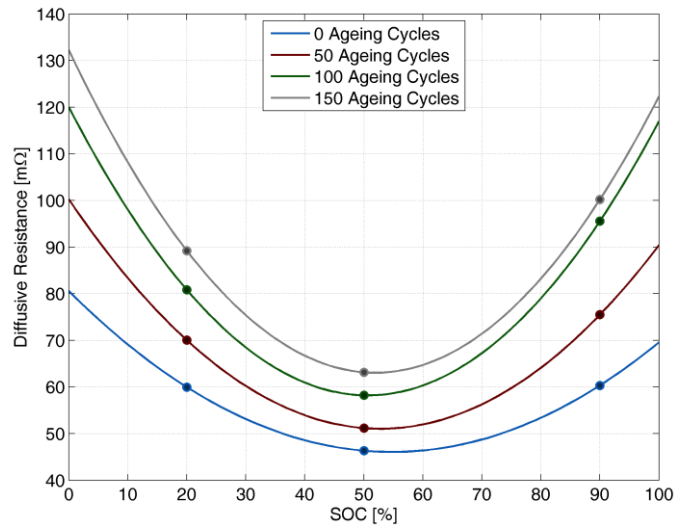


Figure 4: Variation in diffusive resistance with SOC

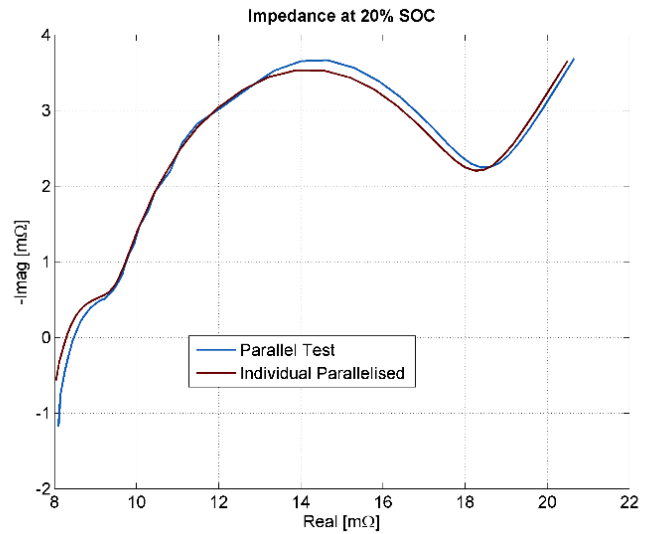


Figure 5: Nyquist plot of experimental and predicted impedance

IV. MODEL FITTING

A nonlinear least squares (NLS) optimization was used to fit an equivalent circuit model, with the cost function vector to minimize given in (9), where v_{exp} and v_{ECM} are the experimental and simulated voltage respectively. The optimization was constrained to prevent negative parameter values and time constants less than the sampling time of the data (10ms).

$$\min \|v_{exp} - v_{ECM}\|_2^2 \quad (9)$$

Figure 6 shows an example of a fit which had an RMS error of 0.61mV and a peak error of 6.6mV. To capture the wide range of responses that can occur between cells in parallel, three RC pairs were used in the model, with time constants of approximately 0.1s, 5s and 60s respectively.

V. RESULTS

Two drive cycles have been considered for this analysis: a dynamic current profile, typical of a hybrid electric vehicle, and a charge-discharge cycle which is more relevant to a battery electric vehicle. Cell connection resistance is ignored for the drive cycle analysis, and discussed separately.

A. Dynamic Current Profile

A drive cycle, representative of a hybrid electric vehicle (HEV) current was simulated using the parallel cell model and the single ECM of the parallel unit. The applied current, cell current (zoomed into a 60s region for clarity) and SOC are shown in Figure 7. As can be seen there is little variation in SOC- a maximum of 0.6% between the cells. The cell currents converged to a steady state in approximately 0.5s after a step change in applied current, suggesting that only the 0.1s time constant was excited. In this steady condition, the DC resistance is the main factor in determining the current through each cell. As a result, the least and most aged cells had a normalized charge throughput of 28% and 22% respectively.

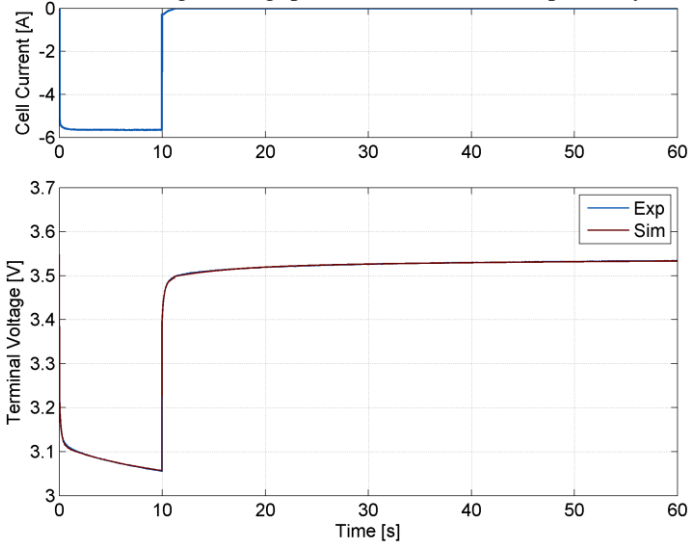


Figure 6: Experimental and simulated voltage response to pulse current

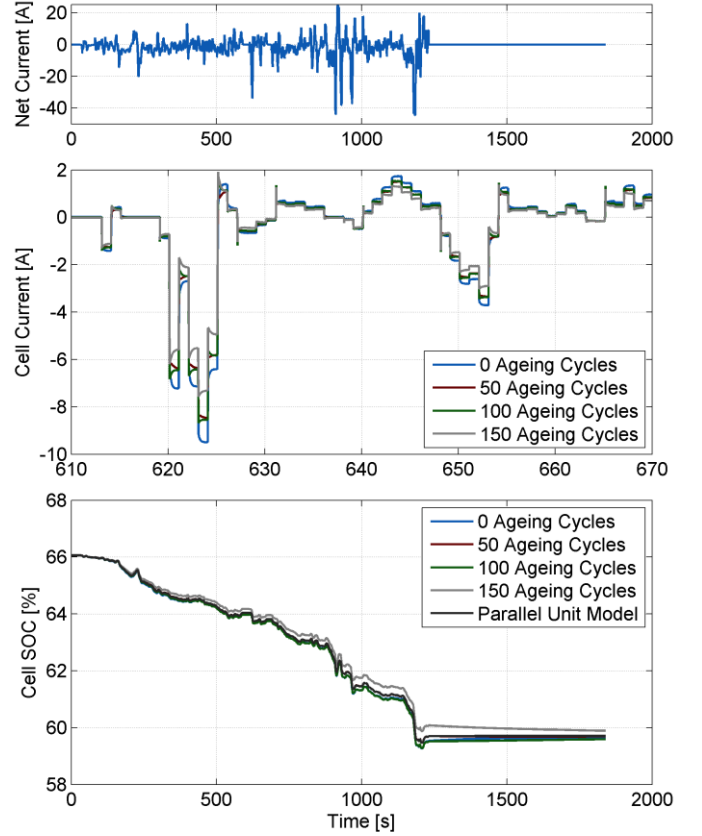


Figure 7: Dynamic drive cycle simulation results

B. Large Depth of Discharge

Unlike HEVs, battery electric vehicles (BEVs) are more likely to cover a large DOD. A simulation of a 2C discharge to the lower voltage limit, followed by a 1C CC-CV charge, was run for both the parallel and single ECM models, with the applied current, cell current and SOC shown in Figure 8. The proportion of charge throughput taken by each cell was more equal than for the dynamic drive cycle, with the least and most aged cells taking 26.5% and 23.5% respectively. However, at the end of discharge the most aged cell had a SOC 5.7% higher than the least aged cell, with the self-balancing of the cells reducing this to under 0.3% after a 15 minute rest period. BMSs may impose limits on upper and lower SOC in order to increase the life of the cell. These results show that it is possible for some individual cells to go outside of this range even though the parallel cell model shows that the parallel unit as a whole is within the limits, potentially decreasing the lifespan of the pack.

OCV also has a significant impact on the performance of the cells for high DOD operation. Under steady state conditions the current through a cell is given by (10).

$$i_{cell} = \frac{V_t - V_{OC}}{R_{DC}} \quad (10)$$

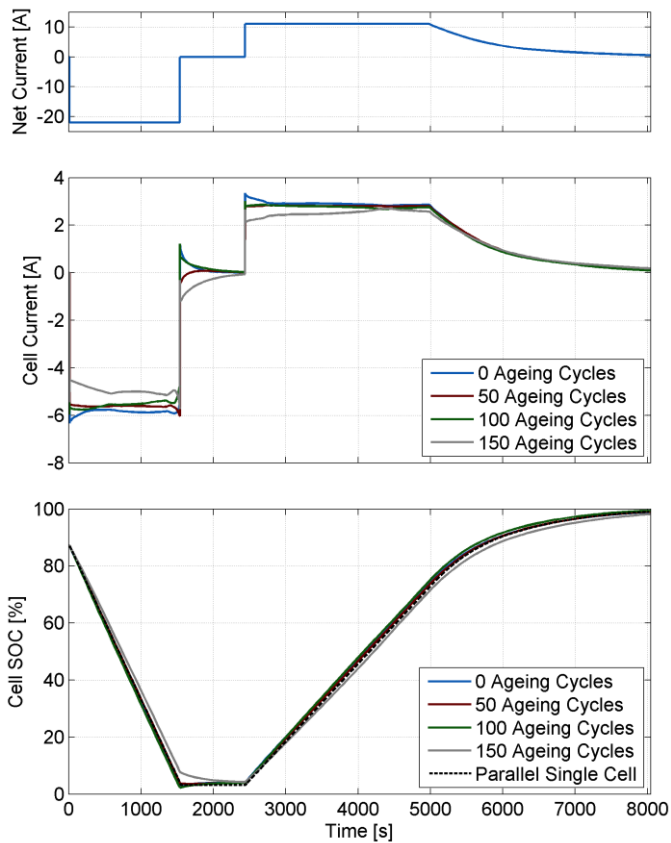


Figure 8: Large DOD simulation results

The OCV curve for this cell is highly nonlinear below 15% SOC. For the discharging case, the OCVs of the more discharged cells becomes closer to the terminal voltage meaning less current is required through the resistor to ensure a common terminal voltage. Cells with a higher OCV must take more of the current until their OCVs also drop.

C. Connection Resistance

Cells in parallel are typically connected together using a high conductivity material such as aluminium [2]. This will create a small additional resistance to the complete parallel assembly. For many cells connected in a ‘ladder’ formation such as in Figure 1, the effect of these resistances becomes significant. Figure 9 shows a 60 second snapshot of the cell currents from the dynamic drive cycle for a model of 70 cells in parallel with identical ECM parameters, but a connection resistance of $10\mu\Omega$ between each cell. The cells closest to the current source (the blue lines on Figure 9) undergo consistently higher loading. This is quantified in Figure 10, which shows the total absolute charge throughput for each cell. The cell nearest to the current source had a 140% charge throughput relative to nominal (the case of no connection resistance), whereas the furthest cell had 85% of the nominal charge throughput. Arguably this significantly higher loading near the current source will cause increased ageing of those cells[4], and may increase demand on the thermal management system due to increase ohmic heating.

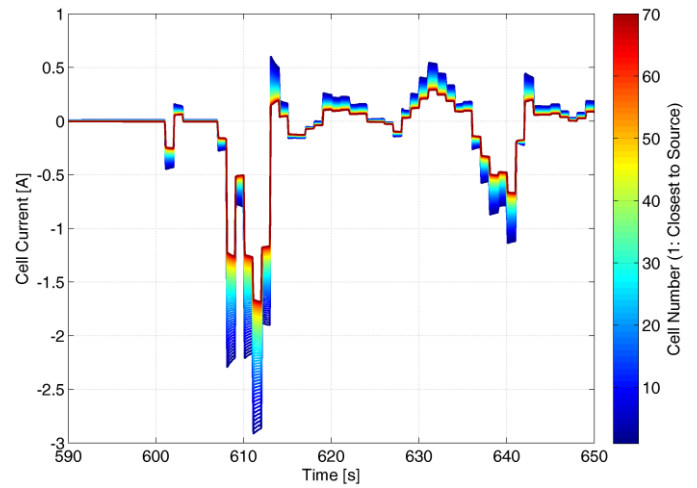


Figure 9: Cell current during drive cycle, with connection resistance

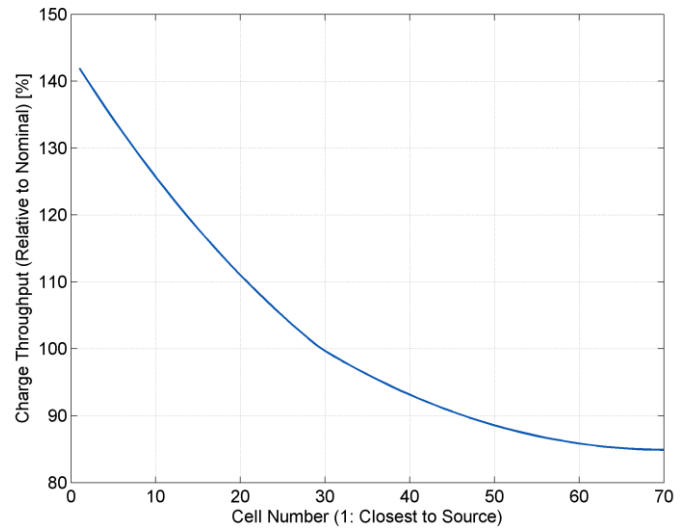


Figure 10: Relative charge throughput of cells in parallel

D. Cell Disconnection

It is possible for cells to lose electrical contact with the battery pack due to vibration and fatigue[10]. For cells in series this means the battery pack as a whole has failed, but for a parallel unit the other cells in the unit are still connected. While the battery pack can still function, the capacity has reduced but the BMS may not be aware of this. In the scenario presented in Figure 11, the least aged cell disconnected after 165s. In this case the drive cycle can no longer be completed due to the cell hitting its lower voltage limit at 909s. The SOC of the cells also decreased more quickly due to the same current having to be spread across one fewer cells. The SOC estimate is likely to become less accurate, especially for a model-based observer such as an extended Kalman filter [11] because its single cell model will have a capacity that is too high and resistance that is too low.

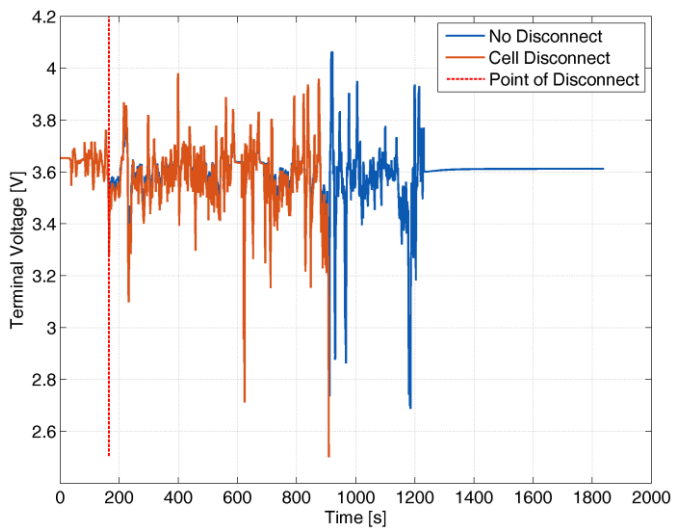


Figure 11: Terminal voltage over a dynamic drive cycle with a disconnected cell

VI. CONCLUSIONS

All of the scenarios assessed in this paper show that cells with different resistances and capacities connected in parallel can undergo significantly different currents. As a BMS does not monitor current within parallel units, some cells may be taken above their intended operating current, or be aged more quickly due to increased charge throughput and ohmic heat generation, shortening the lifespan of the pack. Similarly, a cell losing electrical contact with the battery pack could cause the BMS to overestimate the SOC of the pack, leading to the driver being misled about the available range of the vehicle. A typical HEV drive cycle does not appear to cause a significant amount of SOC variation between cells in parallel due to its dynamic nature. However, steady currents and drive cycles which cover a large DOD, where cells can enter the nonlinear region of the OCV-SOC curve, can cause significant variation and give rise to cases where higher resistance cells can take larger currents. These effects, combined with the cumulative impact of cell connection resistance, can lead to premature ageing of some cells, weakening the pack as a whole. Variation in current can also cause uneven heat generation within a pack which may require a more advanced thermal management system.

ACKNOWLEDGMENTS

The authors would like to thank Neelu Kumari, Dhammika Widanalage and Gael Chouchelamane for their assistance with cell characterization.

REFERENCES

- [1] L. Lu, X. Han, J. Li, J. Hua, and M. Ouyang, "A review on the key issues for lithium-ion battery management in electric vehicles," *J. Power Sources*, vol. 226, no. 0, pp. 272–288, 2013.
- [2] G. J. Offer, V. Yufit, D. A. Howey, B. Wu, and N. P. Brandon, "Module design and fault diagnosis in electric vehicle batteries," *J. Power Sources*, vol. 206, no. 0, pp. 383–392, May 2012.
- [3] J. Kim and B. H. Cho, "Screening process-based modeling of the multi-cell battery string in series and parallel connections for high accuracy state-of-charge estimation," *Energy*, vol. 57, no. 0, pp. 581–599, Aug. 2013.
- [4] A. Barré, B. Deguilhem, S. Grolleau, M. Gérard, F. Suard, and D. Riu, "A review on lithium-ion battery ageing mechanisms and estimations for automotive applications," *J. Power Sources*, vol. 241, no. 0, pp. 680–689, 2013.
- [5] J. Gomez, R. Nelson, E. E. Kalu, M. H. Weatherspoon, and J. P. Zheng, "Equivalent circuit model parameters of a high-power Li-ion battery: Thermal and state of charge effects," *J. Power Sources*, vol. 196, no. 10, pp. 4826–4831, 2011.
- [6] R. Gogoana, M. B. Pinson, M. Z. Bazant, and S. E. Sarma, "Internal Resistance Matching for Parallel-Connected Lithium-Ion Cells and Impacts on Battery Pack Cycle Life," *J. Power Sources*, vol. 252, no. 0.
- [7] X. Gong, R. Xiong, and C. C. Mi, "Study of the characteristics of battery packs in electric vehicles with parallel-connected lithium-ion battery cells," *Applied Power Electronics Conference and Exposition (APEC), 2014 Twenty-Ninth Annual IEEE*. pp. 3218–3224, 2014.
- [8] X. Hu, S. Li, and H. Peng, "A comparative study of equivalent circuit models for Li-ion batteries," *J. Power Sources*, vol. 198, pp. 359–367, Jan. 2012.
- [9] A. Jossen, "Fundamentals of battery dynamics," *J. Power Sources*, vol. 154, no. 2, pp. 530–538, Mar. 2006.
- [10] M. a. Roscher, R. M. Kuhn, and H. Döring, "Error detection for PHEV, BEV and stationary battery systems," *Control Eng. Pract.*, vol. 21, no. 11, pp. 1481–1487, Nov. 2013.
- [11] G. L. Plett, "Extended Kalman filtering for battery management systems of LiPB-based HEV battery packs: Part 1. Background," *J. Power Sources*, vol. 134, no. 2, pp. 252–261, 2004.